Coexistence Evaluation of Densely Deployed BLE-based Body Area Networks

Quang Duy La, Duong Nguyen-Nam, Mao V. Ngo, and Tony Q. S. Quek
Singapore University of Technology and Design, 8 Somapah Road, Singapore 487372
Email: {quang_la, namduong_nguyen, tonyquek}@sutd.edu.sg, vanmao_ngo@mymail.sutd.edu.sg

***Abstract*—In wireless body area network (BAN) applications such as wearable computing, healthcare and sports, Bluetooth Low Energy (BLE) is a new and promising technology, which uses the unlicensed 2.4-GHz spectrum band for data transmission. Since there exist many wireless technologies operating in this frequency band, the issues of cross-technology interference and coexistence present a major challenge. In this work, we develop a testbed to conduct our experimental studies, focusing on BLE and its coexistence capabilities when being deployed in a dense environment, under possible interference from WiFi and ZigBee/IEEE 802.15.4. One scenario of interest is a network of several co-located BLE-based BANs, each of which is designed in a star topology with one gateway and multiple BLE sensor nodes. The second scenario represents a highly heterogeneous network where each BAN now carries both BLE and ZigBee sensors, while being exposed to interference from external WiFi transmission. Our results show that the performance of BLE is relatively robust to interference from other BLE transmissions as well as those from nearby ZigBee and WiFi devices.**

I. Introduction

A. Overview

The widespread development of the Internet-of-Things (IoT) and low-power wireless technologies have led to profound interest in wireless body area networks (BANs). A BAN is composed of multiple nodes of very low-power, short-range sensors, sending and receiving data through wireless technologies. The sensors collect data from their surrounding environments, such as temperature, pressure, humidity or physiological conditions from human body. Primary applications of BANs are in the healthcare domain, e.g., for ubiquitous monitoring of patients with chronic disease such as heart attack; but other use cases include military and sports.

Existing wireless technologies suitable for BANs are Bluetooth, Bluetooth low energy (BLE), or ZigBee/IEEE 802.15.4, which all operate in short-range with low-power. BLE is an emerging technology for short-range communication, developed in the distinctive feature of Bluetooth 4.x specification [1], [2]. Compared to the classic Bluetooth, it offers considerably reduced power and cost consumption. It can also support higher data rate and lower latency than ZigBee [3], [4]. Thus, BLE is a very promising technology for BANs.

The heterogeneous candidate technologies for BANs above share the same frequency bands, i.e., the 2.4-GHz industrial, scientific, and medical (ISM) radio bands, which is notably home to not only Bluetooth, BLE, ZigBee but also WiFi. As shown in Fig. 1, BLE uses 40 narrow-band channels of 2 MHz bandwidth (3 advertising channels and 37 data channels). ZigBee also has narrow-band channels of 2 MHz

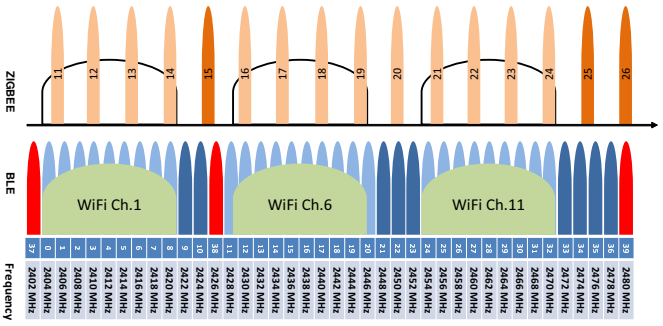

Fig. 1. Spectra of multiple wireless technologies in the 2.4-GHz ISM band

bandwidth with a total of 16 channels spaced by 5 MHz. The WiFi channels are 20 MHz wide and their center carriers are separated by 5 MHz. Channels 1, 6 and 11 are non-overlapping channels and are commonly used for transmission. Cross interferences among multiple wireless technologies will occur due to the crowded shared frequency band. The use of incompatible modulations and channel access schemes makes it difficult to guarantee performance of devices across different technologies. Therefore, it is most important to study their coexistence by considering mutual and cross-technology interferences, especially for the case of BLE.

B. Related Work and Contributions

We look at previous literature on BLE-based BANs and their coexistence. First, there are some works on implementing BLE platform to investigate its features and performances. A BLE platform for remote health monitoring and compatibility for electrocardiography (ECG) monitoring was implemented in [4]. Paper [5] provided experimental data on power consumption of BLE compared to ZigBee and ANT protocols in a cyclic sleep scenario. The authors reported the lowest power consumption for BLE compared to ZigBee and ANT. In [6], a BAN testbed with one master and four slaves was set up for experimental evaluation, but external interferences were not considered. Meanwhile, [7] conducted spectrum survey to investigate the characteristics of BLE system without specifying interference sources, by measuring the BLE transmission failure probability at a sport facility, university food court, and hospital intensive care unit. Results confirmed that BLE is resilient to the presence of high interference.

Cross-technology interferences and coexistence issues for BLE are investigated with other wireless technologies in several previous works. Silva *et al*. [8] conducted interference

tests in an anechoic chamber for a pair of BLE devices, with a single interferer (either WiFi, ZigBee or classic Bluetooth). Siekkinen *et al.* [9] compared the performance of BLE to ZigBee, under WiFi interference. Bronzi *et al.* [10] presented their testbed to study BLE in inter-vehicular communications, with one pair of BLE devices and three pairs of Raspberry Pis in WiFi mode occupying channels 1, 6 and 11. Most of the above works confirmed that BLE is resilient to interference from WiFi as well as ZigBee. However, it is noted that previous works only considered very few devices and did not qualify as a dense deployment. A dense scenario was considered in [11], where the BLE latency and energy consumption under mutual interference were studied for one BLE pair with up to 15 other BLE pairs as interferers. However, this work only focuses on the BLE device discovery phase and does not offer insights during the BLE data transfer phase.

Coexistence in the 2.4-GHz ISM bands, especially for BLE, has attracted a lot of works recently. However, to the best of our knowledge, the following two BAN deployment scenarios are currently lacking in coexistence studies: 1) densely-deployed BANs based on mutual BLE piconets (independent Bluetooth-based star-topology networks); and 2) dense heterogeneous BANs where BLE devices and those of other technologies are deployed simultaneously in the same BAN. These have important implications in modern days, where a large group of co-located people (e.g., in a hospital ward) can carry multiple wearable computing devices, under similar or different wireless interfaces (e.g., patients carrying both ZigBee-based electrocardiogram (ECG) sensor and BLE-based smart-band tracker). In the IoT realm, these heterogeneous devices can interoperate via IPv6 [12] (e.g., the smart trackers could query pulse data from the ECGs for user monitoring). Thus, enabling coexistence and interoperability of heterogeneous devices is necessary to realize the full potential of the IoT, making it imperative to investigate the above two scenarios. We note also that tests and analyses for multiple piconets have been widely reported for classic Bluetooth [13]–[16]; but parallel results are currently lacking for BLE. Motivated by that, our work considers multiple BANs based on BLE and investigates both mutual and heterogeneous networks in terms of BLE coexistence, where WiFi interference can also be present. We conduct extensive experiments via our developed testbed in order to gain insights into the above key challenges. Thus, the contributions of this paper are three-fold:

- Presenting our developed BAN testbed, including the custom BLE-mote as the IPv6 BLE-enabled sensor platform, which is compatible with IoT devices and applications.
- Evaluating the coexistence of densely-deployed BLE-based BANs, with and without WiFi interference.
- Evaluating the coexistence of BLE in dense heterogeneous BANs where BLE and ZigBee are present simultaneously, with and without WiFi interference.

II. Description of the Testbed

A. General Topology

Our testbed consists of several independently deployed BANs in close proximity of each other. A single BAN consists of several body sensor nodes and a gateway node connected in a star topology, which is intended for a single human body. A single BAN may contain sensors with highly heterogeneous functions for different monitoring purposes, including motion, ambiance, vital signs, and so on. The sensors, furthermore, mainly utilize BLE as their means of communications (and occasionally ZigBee). The sensor nodes will transmit their collected data to the gateway; and the gateway is responsible for either processing the data or forwarding the data to a common back-end server for further processing. We allow the gateways to use wired Internet connections to the server in order to focus only on the interferences across different BANs. As heterogeneous nodes content for the available wireless resources to transmit their data, we are interested in their performance under mutual and cross-technology interference.

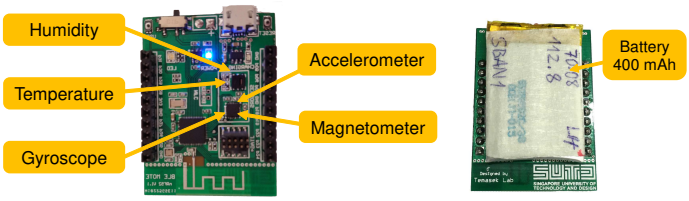

(a) (b)

Fig. 2. The BLE-mote with (a) Front and (b) Back view.

B. Hardware Specification

1) BLE Platform – The BLE-mote: The BLE-mote is a BLE development kit which was developed at Temasek Labs, Singapore University of Technology and Design (SUTD) in 2016. Each BLE-mote is an integrated circuit (IC) board upon which several sensors can be mounted. Fig. 2 shows the layout of a BLE-mote. The BLE-mote board is itself based on Nordic Semiconductor's nRF52832 IC [17].

The BLE-mote has the following specifications:

a) Radio communications: 2.4-GHz transceiver; -96 dBm sensitivity in BLE mode; single-pin antenna interface; 1 - 2 Mbps supported data rates; Tx power: -20 to +4 dBm in 4 dB steps.
b) Microcontroller unit (MCU): ARM® Cortex®-M4 32-bit processor with floating-point unit (FPU), 64 MHz; 512 kB flash memory/64 kB RAM.
c) Built-in Sensors: MPU9250 [18] (triaxial accelerometer, magnetometer and gyroscope); and SHT21 [19] (humidity and temperature) sensor chips.
d) Battery: Polymer Lithium-Ion, 3.7V at 400mAh.

The novel features of the BLE-mote are that it is one of the first development kits that supports BLE ver. 4.2 as well as IPv6 capability as an enabler of the IoT (at the time of writing); and it allows for easy integration of a wide range of off-the-shelf sensor and healthcare devices.

2) Gateway: We choose Raspberry Pi 3 (RPi3) [20] as the hardware device for the gateway. RPi3 is an off-the-shelf single-board computer which supports BLE 4.1. The main advantages of using RPi3 in our testbed are that it allows for adoption of the latest open-source BLE stack in Linux kernel,

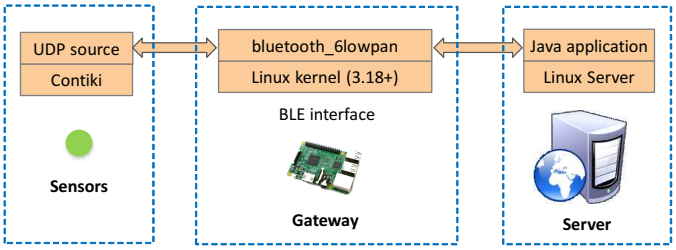

Fig. 3. The testbed's software specification.

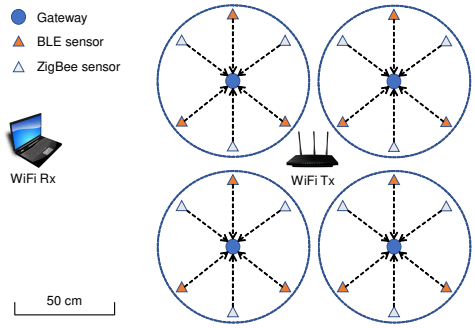

Fig. 4. Schematic of the testbed placement

i.e., the BLE IPv6 over low power wireless personal area networks (6LoWPAN) gateway module; and that this solution follows the IoT standards, which will enable interoperability of the platform with other off-the-shelf IoT products.

C. Software Specification

The diagram in Fig. 3 shows the software interfaces between the different devices within the testbed. For the sensor platform (BLE-motes), the operating system (OS) is Contiki, an open source OS for the IoT [21]. Currently, we are implementing Contiki using the software development kit (SDK) provided directly by Nordic. On the application layer, the BLE-motes run a user datagram protocol (UDP)-sender application to send the packets to the server via the gateway. We use the IPv6 over BLE protocol stack [22], with IPv6 layer on top of BLE 6LoWPAN and BLE logical link control and adaptation protocol (BLE L2CAP).

On the other hand, the RPi3 gateway interfaces with BLE-motes directly via the `bluetooth_6LoWPAN`, which is a module on top of Linux Kernel (version 3.18+), available from open sources. RPi3 then also forwards packets to the remote server, via IPv6/IPv4 Ethernet interface.

The server runs *Collector-View*, a two-part application modified from an open-source framework provided along with Contiki-OS for our purposes. The first part of *Collector-View* runs on sensor platforms, which is implemented in C and utilized to forward measurement data to gateway and server. The second part, implemented in Java, runs on the server site on top of Linux system. It collects sensor data via UDP connection through RPi3 gateway, then visualizes data graphically for analytical purposes.

III. Experimental Setup

A. Scenarios

Our experiments address two main BLE coexistence issues for 1) dense BLE-based BANs; and 2) dense heterogeneous BANs. As such, the following two scenarios are considered:

1) Dense BLE-based BANs: In this scenario, each BAN is an independent BLE piconet, i.e., a star network with a gateway at the center and 3 surrounding BLE-motes at an approximately 0.3 m distance from the gateway. The number of BANs will be varied from 1 to 4. Neighboring BANs are placed within a 0.5 to 2 m distance from each other (measured from the gateway). The whole testbed is placed inside an indoor laboratory and on an even surface (see Fig. 4).

2) Dense heterogeneous BANs: In this scenario, the testbed placement is similar to the previous one and the number of BANs will also be varied from 1 to 4. However, each BAN now not only contains 3 BLE nodes but also 3 other ZigBee nodes simultaneously. The 6 nodes also are placed around a common gateway in a star topology at around 0.3 m distance. Therefore, at maximum capacity, the system can contain up to 24 heterogeneous devices transmitting simultaneously all located within a small area. We use the OpenMote-CC2538 combined with the OpenBattery board [23] as the ZigBee transmitting device, on which various sensors have also been built in, e.g., SHT21 (temperature and humidity), MAX44009 (light) and ADXL346 (accelerometer). One OpenMote-CC2538 device is plugged into the RPi3 gateway via serial port acting as the sink node in order to collect data from other transmitting ZigBee nodes. Time-slotted channel hopping (TSCH) protocol [24] is used as the medium access control (MAC) protocol for ZigBee devices, which is configured to do frequency hopping over a 16-frequency sequence.

Fig. 4 shows a schematic of the testbed placement in the laboratory. For the first scenario, the ZigBee nodes are switched off. We first run the experiment with one BAN switched on, then gradually the other BANs can be added with up to 4 BANs simultaneously.

B. External Interference

Ambience: Our testbed is run under the normal everyday environment of the laboratory. No intentional interferer is present. Any interfering signals in the wireless medium (i.e., the 2.4-GHz band) come from neighboring wireless networks such as the office's wireless local area networks (WLANs). We refer to their presence as the ambience, which will be present in all scenarios and considered a benchmark.

ZigBee/IEEE 802.15.4: In a heterogeneous BAN configuration such as the one used in our second scenario above, both BLE and ZigBee sensors can be carried by the same BAN. However, in the scope of this work, we treat coexisting ZigBee nodes in the same BAN as interferers.

WiFi: A nearby WiFi interferer can be intentionally introduced in order to study the coexistence of our testbed with WiFi networks. We set up a private WLAN through which a laptop downloads a large file from a wireless router. The interferer uses WiFi channel 1 throughout the experiments and the speed limit for downloading is set at 32 Mbps. The

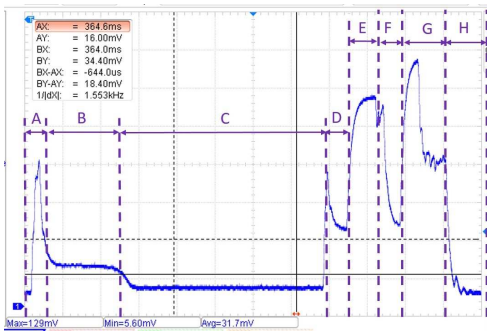

Fig. 5. Current profile of BLE connection event

locations of the WiFi transmitter and receiver relative to the BANs are also depicted in the diagram in Fig. 4. This setup will be applied to both scenarios in Section III-A.

C. Measurement Approach

We will define and detail how to obtain the measurement metrics which will be used to evaluate the system performance.

1) Power Consumption: This directly measures power efficiency, defined as the averaged power consumption in mW of a BLE-mote across the duration of one BLE connection event. Fig. 5 shows our measurement of the current using a 10Ω shunt resistor during a BLE connection event, whose profile is perfectly matched with the one provided by Nordic [17]. The main states of a BLE-mote can be roughly divided into: CPU activity mode (A, B), standby (low power) mode (C, H), Rx mode (D, E) and Tx mode (F, G). The average rated currents of each mode can be obtained from [17]. Specifically, $I_{CPU} = 3.712mA$, $I_{LP} = 1.2\mu A$, $I_{Rx} = 5.3mA$, and $I_{Tx} = 5.4mA$ (these are average values over their whole respective periods). The average voltage is $V = 3V$. Hence, the average power can be computed from the electrical currents, voltage and the measured time ticks in software, as follows:

$$P = \frac{V(I_{CPU}T_{CPU} + I_{LP}T_{LP} + I_{Rx}T_{Rx} + I_{Tx}T_{Tx})}{T_{CPU} + T_{LP} + T_{Rx} + T_{Tx}}. \quad (1)$$

2) Radio Duty Cycle (RDC): RDC measures the percentage of time the radio module of the device is on, in percentage (%). RDC enables fair comparison of protocols across hardware platforms [12], which may have different clocking profiles but similar timing of radio transmission. It is given by

$$\text{RDC} = \frac{T_{Rx} + T_{Tx}}{T_{CPU} + T_{LP} + T_{Rx} + T_{Tx}}. \quad (2)$$

3) UDP Packet Delivery Ratio (PDR): We use the UDP packet delivery ratio as a metric for reliability. PDR, measured in percentage (%), is defined as the percentage of UDP packets successfully delivered from the sender (BLE-mote) to the receiver (back-end server). Specifically, we count number of UDP packets received at the back-end server and track the consecutive sequence number of these packets to capture missing packets over time. Let N_{UDP} and $\mathsf{N}^*_{\text{UDP}}$ be the total number of transmitted UDP packets and successful UDP packets, respectively. Then, the PDR is given by

$$\text{PDR} = \frac{\mathsf{N}^*_{\text{UDP}}}{\mathsf{N}_{\text{UDP}}}. \quad (3)$$

4) BLE Packet Reception Ratio (PRR): PRR is a measure of one-hop communication between the BLE-mote and the gateway from a link-layer perspective. PRR is defined as the percentage of BLE packets successfully received from a BLE-mote at the RPi3. The number of BLE packets is not the same as the number of UDP packets; thus PRR and PDR are two different measures. The reasons for having these two separate ratios are not only layer-dependent but also to account for one-hop vs. end-to-end communications (e.g., two separate ratios are considered in [25]). Also, BLE retransmissions are not reflected in PDR at higher layer but can be captured by PRR; hence PRR usually has smaller values. Similarly, let N_{BLE} and $\mathsf{N}^*_{\text{BLE}}$ be the total number of transmitted BLE packets by BLE-motes and the number of successful BLE packets at the respective gateways, respectively. Then, the PRR is given by

$$\text{PRR} = \frac{\mathsf{N}^*_{\text{BLE}}}{\mathsf{N}_{\text{BLE}}}. \quad (4)$$

D. Parameters

For each combination of network topologies and interferers, an experiment lasts for *two hours*. The various measurement metrics of interest will be recorded and logged at the server. At the end of an experiment, statistics such as power consumption, RDC, PDR for UDP packets and PRR for BLE packets are averaged over all individual nodes. For all the nodes, transmission power is set at *0 dBm*.

The amount of data to be collected by nodes and transferred back to the server is usually application-dependent. In this work, we consider data from accelerometer sensors, which can have applications such as in healthcare and patient activity monitoring. Thus, the data payload consists of samples from the triaxial accelerometer of each sensor node. On each accelerometer, 6 bytes of data will be collected per sample (3 axes × 2 bytes/axis). With the default sensor's sampling rate of 32Hz, this amounts to *192 bytes of payload* generated per second. The *sending rate* (i.e., rate at which new UDP packets are sent to the gateway by sensors) is set at *6 Hz*. That is, each UDP packet contains $\frac{192}{6} = 32$ bytes of application data.

For BLE, apart from application data, a UDP packet also contains IPv6 header of 32 bytes. With the Nordic BLE stacks, each BLE packet can carry only 27 bytes of data. Therefore, it takes $\lceil \frac{32+32}{27} \rceil = 3$ BLE packets to transmit one UDP packet; or 18 BLE packets per second. For ZigBee, the 32 bytes can fit into one IEEE 802.15.4 packet (at PHY/MAC layer), which can contain up to 127 bytes of data. Therefore, 4 IEEE 802.15.4 packets per second can be sent to the gateway.

IV. Experimental Results

Using the measurement approach and the testbed setup described above, we perform our coexistence experiments for each scenario. We allow the number of BANs to vary from 1 to 4; and each configuration is subject to both with and without WiFi interference. The results of the coexistence experiments are shown in Figs. 6 to 9.

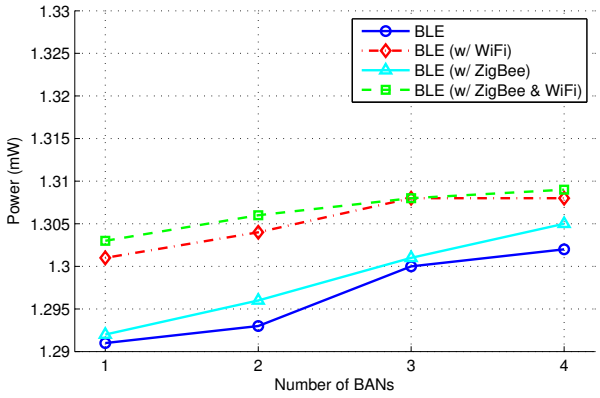

Fig. 6. Average power consumption of BLE nodes vs. the number of BANs

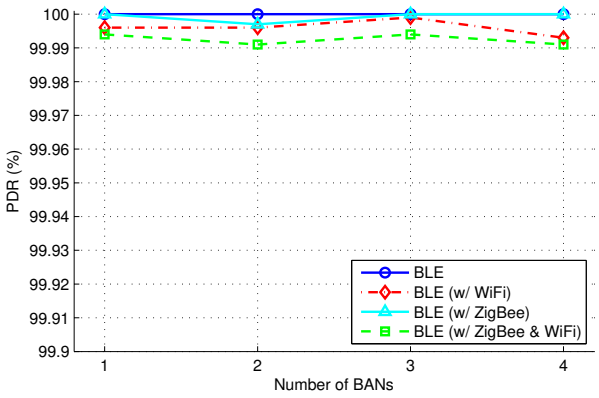

Fig. 8. Average UDP packet delivery ratio vs. the number of BANs

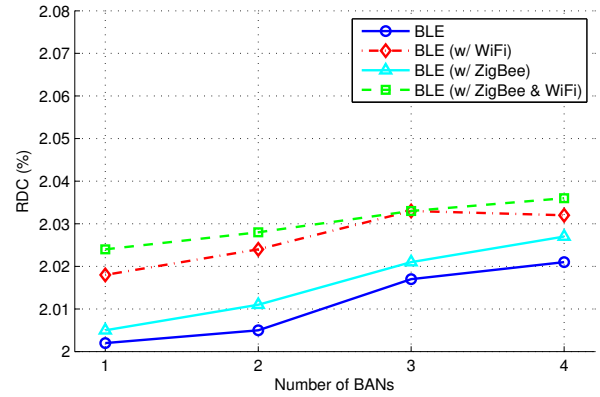

Fig. 7. Average radio duty cycle of BLE nodes vs. the number of BANs

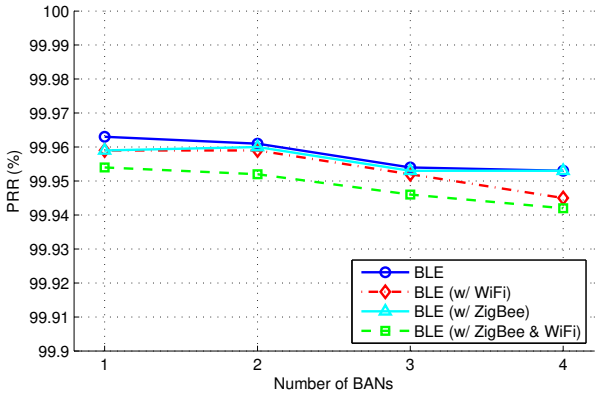

Fig. 9. Average BLE packet reception ratio vs. the number of BANs

1) Power Consumption: The measurement results for average power consumption of BLE nodes are collected and displayed in Fig. 6 against the number of BANs. The results are further divided into 4 groups: BLE-based BANs, with and without WiFi interference; and BLE in heterogeneous BANs (with ZigBee), with and without WiFi interference. They are abbreviated by *BLE*, *BLE (w/ WiFi)*, *BLE (w/ ZigBee)* and *BLE (w/ ZigBee & WiFi)*, respectively.

Our first observation is that as the number of BANs increases, power consumption also grows in all groups, although the margin is relatively small. On average, each BLE node in the 1-BAN ambient case consumes about 1.291 mW. When the number of BANs goes up to 4, this figure only increases to 1.302 mW, i.e., by 0.85%. Similar figures can be seen with the other cases. It is thus implied that when the network is denser, nodes should engage more in radio transmission, possibly as more collisions and retransmissions occur, causing power consumption to increase. We should therefore see the same trend in RDC in Fig. 7, which will be discussed later.

Regarding the impacts of interferers on BLE power consumption, the results in Fig. 6 seem to indicate that both ZigBee and WiFi presences cause BLE to spend more power; and the effect of WiFi interference is more apparent. In fact, for the dense BLE-piconet BANs (marked by circles and diamonds), introducing WiFi causes a 0.009 mW power jump on average; and for the heterogeneous BANs (marked by triangles and squares), 0.008 mW. Meanwhile, by introducing ZigBee simultaneuously with BLE, the above figures are reduced to 0.002 mW and 0.001 mW, respectively. Nevertheless, the amount of average power increment is relatively tiny. Thus, our data, to some extent, have verified that BLE is relatively resilient to dense deployment as well as cross-technology interference, in terms of power consumption.

To further put things into perspective, we also compare the average BLE power with that of ZigBee nodes, which is around 6.093 mW (not shown in the figures), i.e., 4.7 times higher than BLE's. This suggests that BLE is highly more power efficient compared to ZigBee. The result is in line with previous findings which showed a superior energy efficiency of BLE over ZigBee [5], [9].

2) Radio Duty Cycle: The measurement results for RDC are displayed in Fig. 7. The grouping for RDC is similar to those of power consumption in the previous section. We can see from Fig. 7 that RDC shows a remarkably strong correlation to power consumption, as is expected. RDC also grows slightly with the number of BANs; and introducing interference, especially WiFi, also accounts for a higher percentage in the duty cycle. This is also due to the growth in collisions and retransmissions, leading to more time spent in radio modes, similar to the one observed in power consumption. We should

note that the average percentage of RDC in all cases stays roughly above 2% which takes a very small proportion of one BLE connection event. Our RDC results could be compared to those of [12] where RDCs of 0.5-1.3% were recorded for request-response mode and 28.8% for bulk transmission mode. In contrast, our scenarios could be categorized as *periodic traffic* mode due to the constant stream of sensor data, which should lie in between the two cases above.

3) UDP Packet Delivery Ratio: Fig. 8 displays the PDR versus the number of BANs. Overall, PDR measurements are consistently high in all cases, at above 99.99%, and even at 100% for BLE without interferers. This shows that for BLE, delivery of the application payloads can be done reliably even in the presence of dense neighboring devices as well as various cross-technology interference. This might be attributed to the BLE retransmission mechanism, so that even if a collision occurs at the link layer and a BLE packet is lost, it is still possible for the entire UDP packet to be successfully received at the server. The presence of WiFi causes some slight drop in PDR ($< 0.01\%$) over the 2-hour experiments, which is relatively insignificant and comparable to results in [10] (in [10] only 1-minute experiments were reported).

4) BLE Packet Reception Ratio: Fig. 9 displays the PRR results. It first suggests that there are more collisions and packet losses in the link layer than for UDP packets (although the success ratios are still above 99.9%). Collisions seem to occur more often as the spectrum gets congested due to increased number of interfering devices but the PRR degradation is not overall severe. We note that at our sending rate of 18 BLE packets/s, the results show marked PRR improvement over equivalent results [4]. Also, the separation among multiple test scenarios is not clear-cut, confirming the BLE performance robustness in crowded scenarios, with and without cross-technology interference.

V. Conclusions

BLE technology has a huge potential in body-area network applications such as wearable computing, public healthcare and sports. In this work, we develop our own testbed in order to study the coexistence issues of BLE-based BANs in several densely-deployed scenarios, subject to possible cross-technology interference. We also consider a heterogeneous BAN setup with ZigBee nodes and BLE nodes in the same BAN. Through extensive testbed experiments, we measure the average power consumption, radio duty cycle, UDP packet delivery ratio and BLE packet reception ratio and our results have suggested good coexistence capability of BLE, not only in a dense network of mutual BLE-based BANs, but also in a highly heterogeneous setting, under WiFi interference. In the future, our investigation will be extended to include real-time measurements on the human bodies as well as the effect of mobility on the testbed performance.

References

[1] Bluetooth SIG, "The Bluetooth Core specification, v4.0," The Bluetooth Special Interest Group, Tech. Rep., 2010.

[2] R. Tabish, A. B. Mnaouer, F. Touati, and A. M. Ghaleb, "A comparative analysis of BLE and 6LoWPAN for U-HealthCare applications," in *Proc. IEEE-GCC Conference and Exhibition (GCCCE)*, 2013, pp. 286–291.

[3] E. Georgakakis, S. A. Nikolidakis, D. D. Vergados, and C. Douligeris, "An analysis of Bluetooth, Zigbee and Bluetooth Low Energy and their use in WBANs," in *Wireless Mobile Communication and Healthcare*, J. C. Lin and K. S. Nikita, Eds. Springer Verlag, 2011, pp. 168–175.

[4] F. Touati, O. Erdene-Ochir, W. Mehmood, A. Hassan, A. B. Mnaouer, B. Gaabab, M. F. A. Rasid, and L. Khriji, "An Experimental Performance Evaluation and Compatibility Study of the Bluetooth Low Energy Based Platform for ECG Monitoring in WBANs," *Int. J. Distrib. Sen. Netw.*, pp. 1–12, Jan. 2015.

[5] A. Dementyev, S. Hodges, S. Taylor, and J. Smith, "Power consumption analysis of Bluetooth Low Energy, ZigBee and ANT sensor nodes in a cyclic sleep scenario," in *Proc. IEEE IWS*, 2013, pp. 1–4.

[6] J. A. Afonso, A. J. Maio, and R. Simoes, "Performance Evaluation of Bluetooth Low Energy for High Data Rate Body Area Networks," *Wirel. Pers. Commun.*, vol. 90, no. 1, pp. 121–141, Sep. 2016.

[7] M. O. A. Kalaa, W. Balid, N. Bitar, and H. H. Refai, "Evaluating Bluetooth Low Energy in realistic wireless environments," in *Proc. IEEE WCNC*, 2016, pp. 1–6.

[8] S. Silva, S. Soares, T. Fernandes, A. Valente, and A. Moreira, "Coexistence and interference tests on a Bluetooth Low Energy front-end," in *Proc. IEEE Sci. Info. Conf. (SAI)*, 2014, pp. 1014–1018.

[9] M. Siekkinen, M. Hiienkari, J. K. Nurminen, and J. Nieminen, "How low energy is Bluetooth Low Energy? comparative measurements with Zigbee/802.15.4," in *Proc. IEEE WCNC Workshops*, 2012, pp. 232–237.

[10] W. Bronzi, R. Frank, G. Castignani, and T. Engel, "Bluetooth Low Energy performance and robustness analysis for Inter-Vehicular Communications," *Ad Hoc Netw.*, vol. 37, no. P1, pp. 76–86, Feb. 2016.

[11] J. J. Treurniet, C. Sarkar, R. V. Prasad, and W. d. Boer, "Energy Consumption and Latency in BLE Devices under Mutual Interference: An Experimental Study," in *Proc. IEEE Future Internet of Things and Cloud (FiCloud)*, 2015, pp. 333–340.

[12] P. Narendra, S. Duquennoy, and T. Voigt, "BLE and IEEE 802.15.4 in the IoT: Evaluation and Interoperability Considerations," in *Internet of Things. IoT Infrastructures: Second International Summit, IoT 360° 2015, Rome, Italy, October 27-29, 2015, Revised Selected Papers, Part II*, B. Mandler, *et al.*, Ed. Springer, 2016, pp. 427–438.

[13] A. Arumugam, A. Nix, P. Fletcher, S. Armour, and B. Lee, "Scenario driven evaluation and interference mitigation proposals for Bluetooth and high data rate Bluetooth enabled consumer electronic devices," *IEEE Trans. Consum. Electron.*, vol. 48, no. 3, pp. 754–764, Aug. 2002.

[14] I. Howitt, "Mutual interference between independent Bluetooth piconets," *IEEE Trans. Veh. Technol.*, vol. 52, no. 3, pp. 708–718, May 2003.

[15] T.-Y. Lin and Y.-C. Tseng, "Collision analysis for a multi-Bluetooth picocells environment," *IEEE Commun. Lett.*, vol. 7, no. 10, pp. 475–477, 2003.

[16] F. Mazzenga, D. Cassioli, P. Loreti, and F. Vatalaro, "Evaluation of packet loss probability in Bluetooth networks," in *Proc. IEEE ICC*, vol. 1, 2002, pp. 313–317.

[17] Nordic Semiconductor. nRF52832 product specification v1.1. [Online]. Available: http://infocenter.nordicsemi.com/pdf/nRF52832_PS_v1.1.pdf

[18] InvenSense Inc. MPU-9250 Product Specification Revision 1.0. [Online]. Available: http://store.invensense.com/datasheets/invensense/MPU9250REV1.0.pdf

[19] Sensirion. Datasheet SHT21. [Online]. Available: www.sensirion.com/fileadmin/user_upload/customers/sensirion/Dokumente/2_Humidity_Sensors/Sensirion_Humidity_Sensors_SHT21_Datasheet_V4.pdf

[20] Raspberry Pi (Trading) Ltd. Compute module datasheet. [Online]. Available: www.raspberrypi.org/documentation/hardware/computemodule/RPI-CM-DATASHEET-V1_0.pdf

[21] Contiki: The Open Source OS for the Internet of Things. [Online]. Available: http://contiki-os.org/

[22] Internet Engineering Task Force (IETF). (2015) IPv6 over BLUETOOTH(R) Low Energy. [Online]. Available: http://tools.ietf.org/pdf/rfc7668

[23] OpenMote-CC2538 platform. [Online]. Available: www.openmote.com/

[24] IEEE Computer Society, "IEEE standard for local and metropolitan area networks–part 15.4: Low-rate wireless personal area networks (LR-WPANs) amendment 1: MAC sublayer," *IEEE Std. 802.15.4e-2012 (Amendment to IEEE Std. 802.15.4-2011)*, pp. 1–225, Apr. 2012.

[25] J. Ko, J. Eriksson, N. Tsiftes, S. Dawson-Haggerty, A. Terzis, A. Dunkels, and D. Culle, "ContikiRPL and TinyRPL: Happy Together," in *Proc. Workshop on Extending the Internet to Low Power and Lossy Networks (IPSN 2011)*, 2011.